Electrical Drive in/around Torsional Resonance: Analytical Model

D. Pejovski, A. Di Gerlando, G. M. Foglia, R. Perini

***Abstract* – In this paper a complete analytical model of an electric drive in/around torsional resonance is presented. The model includes the electrical equations of a permanent magnet synchronous machine (PMSM), the mechanical characteristics represented by a two-degree-of-freedom (2DOF) system and the equations describing the control system. The objective is to obtain formulae on hand to predict both the electromagnetic and the shaft torque harmonics around resonance. Accounting for the various aspects, this model reveals the interconnections between electromagnetic, mechanical and control phenomena. The overall system solution is obtained by applying the small variations method and transfer functions formalism. The results are confirmed by simulations in Matlab/Simulink environment.**

***Index Terms*—torsional vibrations, PI-control, torque harmonic amplitude.**

I. Nomenclature

R, L	PMSM phase resistance and inductance [Ω], [H]
Ψ_{PM}	permanent magnet flux [Wb]
J_m, J_L	motor and load inertia [kg·m^2]
θ_m, θ_L	motor and load mech. angular position [rad]
$\dot{\theta}_m$, $\dot{\theta}_L$	motor and load mechanical speed [rad/s]
$\dot{\theta}$	motor electrical speed [rad/s]
ψ_d, ψ_q	flux linkage along the dq-axes [Wb]
p	time derivative [s^{-1}]
n_p	number of pole pairs
B	coupling damping [Nms/rad]
K	coupling stiffness [Nm/rad]
T_{sw}, f_{sw}	switching period and frequency [s], [Hz]
k_{pI}	proportional coeff. of the current regulator [V/A]
k_{iI}	integral coeff. of the current regulator [Vrad/As]
$k_{p\Omega}$	proportional coeff. of the speed reg. [Nms/rad]
$k_{i\Omega}$	integral coeff. of the speed regulator [Nm]
$\dot{\theta}_m^{ref}$	reference motor mechanical speed [rad/s]
i_{dq}^{ref}, i_{dq}	reference and actual dq-currents [A]
e_{idq}	error between ref. and measured dq-currents [A]
e_Ω	error between ref. and measured speed [rad/s]
V_h	amplitude of phase voltage harmonic, rms [V]
h_v, h	voltage and torque harmonic order
$f_{c,I}$	current loop cutoff frequency [Hz]
m_f	frequency modulation index
ω_h	harmonic angular frequency [rad/s]
$f_{N,mech}$	natural frequency of the mechanical system [Hz]
f_N	natural frequency of the overall system [Hz]
$\bar{v}_{\alpha\beta(1)}$	fundamental voltage in αβ-frame [V]
$\bar{v}_{\alpha\beta(h)}$	voltage harmonic in αβ-frame [V]
$\bar{\imath}_{\alpha\beta}$	motor currents in αβ-frame [A]
$\bar{\psi}_{\alpha\beta}$	PMSM flux in αβ-frame [Wb]
T_{em} T_L T_{sh}	electromagnetic, load and shaft torque [Nm]
T_{em}^{ref}	reference electromagnetic torque [Nm]

Authors are with the Department of Energy at Politecnico di Milano, Via La Masa 34, 20156 Milano, Italy.
e-mails: dejan.pejovski@polimi.it, antonino.digerlando@polimi.it, gianmaria.foglia@polimi.it, roberto.perini@polimi.it.

II. Introduction

THE control system is an essential part of any modern electric drive since it provides a desired way of machine operation. Its role is particularly important in transient conditions when mechanical oscillations are reflected significantly on the electrical side. Numerous publications have treated the electro-mechanical interactions in an electric drive, and others the effect of the control system on the electrical quantities. To the authors' best knowledge, there is no research that deals with all these aspects in/around resonance condition and combines them in a unique all-inclusive mathematical model which highlights the interconnections among relevant quantities.

In [1], the traditional mechanical lumped-inertia model is extended by a torsional spring and a damper between the motor and the ground to account for the electromagnetic phenomena in the air gap. The results show a shift in the torsional frequencies due to the electrical aspect of the system. The model is verified by multi-physics simulation software, but not experimentally. In [2], the propagation of harmonics resulting from mechanical dynamics to the motor air gap on the electrical side is analysed in detail. The paper provides a very solid basis for further research. In [3], an in-depth analysis of the mechanical system characteristics and torsional vibrations excited by electromagnetic torque harmonic is presented. However, the previous articles do not examine the effect of the control system on the torque harmonics amplitude. In [4], a dynamic model of an integrated electrical drive system is presented, and the electromechanical coupling characteristics are studied. The control system, instead, is analysed separately and the PI speed controller parameters are chosen through multiple simulations. Another paper investigates the effect of the motor flux harmonics due to the slots, current measurement errors and dead time of the inverter. However, it does not consider the detailed mechanical model [5].

In [6], an extensive survey regarding the effect of parameters uncertainties on the torsional frequencies is presented. However, the paper considers mechanical characteristics only, not the electrical ones. In [7], the response of the control system on torsional vibrations is discussed, highlighting the effect of the oscillations present in the measured signals, delays caused by sampling times and calculations inside the control loops. However, this work

does not provide a full mathematical model integrating the control system with the electro-mechanical interactions.

In the industry, a PI speed regulator is typically used for controlling an elastically coupled load. The main issue with this control method is the limited possibility for pole placement and therefore, a limited speed control dynamics. [8]. As suggested in [9], the conventional PI speed loop bandwidth can be reduced to suppress any excitation at the resonant frequency. The problem with this solution is the slow dynamic performance. It should be noted that in many papers dealing with torsional vibrations the inner current loop is assumed to be much faster than the outer speed loop, thus it is represented as a first order lag or a unity gain [10]. This approach loses the dynamics of the inverter and the electrical motor parameters; therefore, it cannot provide a complete picture of the overall system behaviour and the mutual interactions.

In Section III of this paper, the electrical equations of a PMSM in the dq-frame are extended to account for a voltage harmonic generated by the inverter operation. It causes harmonic currents, which, in turn, generate harmonic torques and consequently, mechanical oscillations. When the frequency of a torque harmonic matches the system natural frequency, a torsional resonance is excited. Moreover, in this section the mechanical characteristics of the motor and its load are given by differential equations for a 2DOF system. The control system is also described by appropriate equations. A general all-inclusive model is created in the Laplace domain. The system is solved by applying the small variations method and the resulting transfer functions are combined in the frequency domain to obtain simple formulae for computing the amplitude of the electromagnetic and the shaft torque harmonic in/around resonance. In Section IV, the analytical results are verified by extensive Matlab/Simulink simulations in various operating conditions. Conclusions are presented in Section V.

III. Analytical Model of the PMSM Drive

A general representation of the system under study is shown in Fig. 1. What is important to be highlighted is the formally injected harmonic $\bar{v}_{\alpha\beta(h_v)}$ which in practice appears due to the modulator. In this section each of the blocks in Fig. 1 is modelled separately and then the overall system model is established and solved.

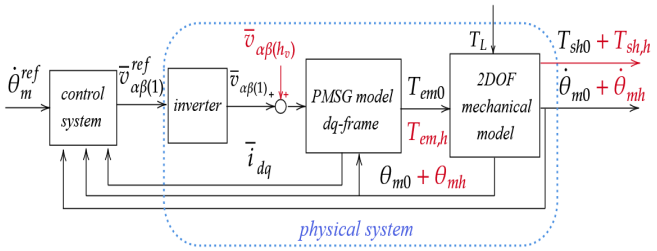

Fig. 1. Basic block-diagram of the system under analysis. Important variables are highlighted in red. Subscripts 0 and *h* or h_v indicate steady-state value and harmonic variation, respectively.

A. Physical System

The physical part of the system consists of the inverter, the PMSM and its load. Let us start from the equations of the machine in the stationary αβ-frame, emphasizing the voltage harmonic $\bar{v}_{\alpha\beta(h_v)}$:

$$\bar{v}_{\alpha\beta(1)} + \bar{v}_{\alpha\beta(h_v)} = R\bar{\imath}_{\alpha\beta} + p\bar{\psi}_{\alpha\beta} \tag{1}$$

In the rotating dq-frame instead, (1) gives rise to the following components along the axes:

$$\begin{cases} v_{d(1)} + v_{d(h)} = Ri_d + p\psi_d - \dot{\theta}\psi_q \\ v_{q(1)} + v_{q(h)} = Ri_q + p\psi_q + \dot{\theta}\psi_d \end{cases} \tag{2}$$

where $h = h_v \pm 1$, according to the harmonic sequence and the fluxes ψ_{dq} are defined as:

$$\begin{cases} \Psi_d = Li_d + \Psi_{PM} \\ \Psi_q = Li_q \end{cases} \tag{3}$$

Applying the small variations method, the system in (2) can be linearised and decomposed to a steady-state value in (4) and an oscillation given in (5):

$$\begin{cases} v_{d0(1)} = Ri_{d0} - \dot{\theta}_0\psi_{q0} \\ v_{q0(1)} = Ri_{q0} + \dot{\theta}_0\psi_{d0} \end{cases} \tag{4}$$

$$\begin{cases} \Delta v_d = \Delta v_{d(1)} + v_{d(h)} = \\ \qquad R\Delta i_d + p\Delta\psi_d - \dot{\theta}_0\Delta\psi_q - \psi_{q0}\Delta\dot{\theta} \\ \Delta v_q = \Delta v_{q(1)} + v_{q(h)} = \\ \qquad R\Delta i_q + p\Delta\psi_q + \dot{\theta}_0\Delta\psi_d + \psi_{d0}\Delta\dot{\theta} \end{cases} \tag{5}$$

The time derivative of the flux variations along the dq-axes are expressed from (5):

$$\begin{cases} p\Delta\psi_d = \\ \qquad -\frac{R}{L}\Delta\psi_d + \dot{\theta}_0\Delta\psi_q + \psi_{q0}\Delta\dot{\theta} + \Delta v_{d(1)} + v_{d(h)} \\ p\Delta\psi_q = \\ \qquad -\dot{\theta}_0\Delta\psi_d - \frac{R}{L}\Delta\psi_q - \psi_{d0}\Delta\dot{\theta} + \Delta v_{q(1)} + v_{q(h)} \end{cases} \tag{6}$$

On the other hand, the mechanically related variables, like angular position and speed, are presented in Fig. 2. They are found from the Newton's equations of motion as in (7) [11], which account for the inertias and the coupling parameters. A 2DOF mechanical system whose data are given in Appendix I is characterised by a torsional frequency $f_{N,mech}$ = 112Hz.

$$\begin{cases} J_m s^2\theta_m = T_{em} - K(\theta_m - \theta_L) - B(\dot{\theta}_m - \dot{\theta}_L) \\ J_L s^2\theta_L = K(\theta_m - \theta_L) - B(\dot{\theta}_m - \dot{\theta}_L) - T_L \end{cases} \tag{7}$$

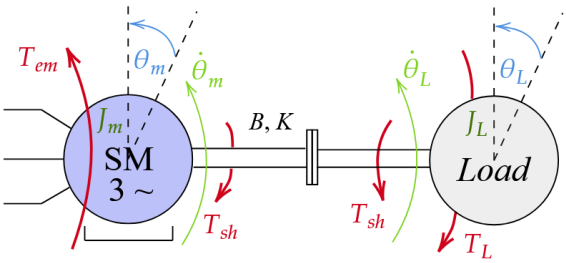

Fig. 2. Mechanical aspects of a 2DOF system consisting of a PMSM, its load and their coupling.

To investigate the effect of T_{em} harmonics on the motor speed, we can consider a constant load torque T_L without any variations and neglect it in the further small signal analysis. The transfer function from the electromagnetic torque T_{em} to the motor electrical speed $\dot{\theta}$ can be obtained from (7) as:

$$\frac{\dot{\theta}}{T_{em}} = \frac{n_p(J_L s^2 + Bs + K)}{J_m J_L s^3 + B(J_m + J_L)s^2 + (J_m + J_L)Ks} = \frac{n_p N(s)}{D(s)} \tag{8}$$

From an electrical point of view, T_{em} is proportional to the flux ψ_q, as given in (9). By introducing it in (8) and applying the small variations method, the time derivative of the electrical speed variation is found as in (10):

$$T_{em} = n_p \Psi_{PM} \psi_q / L \tag{9}$$

$$s\Delta\dot{\theta} = \frac{\psi_{PM}}{L} n_p^2 \frac{J_L s^2 + Bs + K}{J_m J_L s^2 + B(J_m + J_L)s + K(J_m + J_L)} \Delta\psi_q \tag{10}$$

The inverter is commonly represented as a unity gain, or more precisely as:

$$\Delta\bar{v}_{dq} = \frac{1}{1+sT_{sw}} \Delta\bar{v}_{dq}^{ref} \tag{11}$$

B. Control system

Although the block scheme of the control system can be easily found in literature, here it is shown in Fig. 3 since it will be used for defining several relevant equations. The oscillations of the speed and the angular position are put in evidence.

The scheme consists of inner current loop and outer speed loop, both employing PI regulators. Each regulator gives rise to two equations: a differential as in (12) and an algebraic one as in (13):

$$\begin{cases} p\varepsilon_{id} = i_d^{ref} - i_d \\ p\varepsilon_{iq} = i_q^{ref} - i_q \\ p\varepsilon_{\Omega} = \dot{\theta}_m^{ref} - \dot{\theta}_m \end{cases} \tag{12}$$

$$\begin{cases} v_d^{ref} = k_{pI}(i_d^{ref} - i_d) + k_{iI}\varepsilon_{id} - n_p\dot{\theta}_m L i_q \\ v_q^{ref} = k_{pI}(i_q^{ref} - i_q) + k_{iI}\varepsilon_{iq} + n_p\dot{\theta}_m(\psi_{PM} + L i_d) \\ T_{em}^{ref} = k_{p\Omega}(\dot{\theta}_m^{ref} - \dot{\theta}_m) + k_{i\Omega}\varepsilon_{\Omega} \end{cases} \tag{13}$$

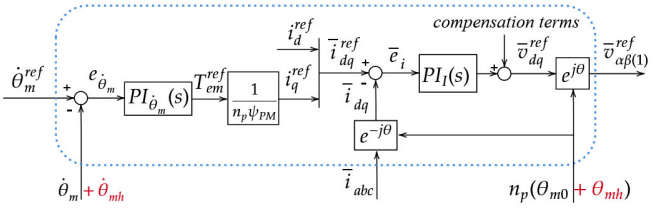

Fig. 3. Block diagram of the control system. Harmonics due to the mechanical oscillations are highlighted in red.

All the compensation terms are included in (13). Another equation can be written from the block-diagram in Fig. 3:

$$T_{em}^{ref} = n_p\psi_{PM} i_q^{ref} \rightarrow i_q^{ref} = \frac{1}{n_p\psi_{PM}} T_{em}^{ref} \tag{14}$$

The small variations method is applied to (12)-(14), having in mind that $\Delta x \cdot \Delta y$ is negligibly small, $\Delta i_d^{ref} = 0$ (assuming MTPA operation) and $\dot{\theta}_m^{ref} = 0$. Substituting the variations of (13) and (14) in (11), we obtain $\Delta v_{d(1)}$ and $\Delta v_{q(1)}$ to be inserted in (6):

$$\Delta v_{d(1)} = \frac{1}{1+sT_{sw}}[k_{pI}(\Delta i_d^{ref} - \Delta i_d) + k_{iI}\Delta\varepsilon_{id} - n_p L\dot{\theta}_{m0}\Delta i_q - n_p L i_{q0}\Delta\dot{\theta}_m] \tag{15.1}$$

$$\Delta v_{q(1)} = \frac{1}{1+sT_{sw}}[k_{pI}(\Delta i_q^{ref} - \Delta i_q) + k_{iI}\Delta\varepsilon_{iq} + n_p\psi_{PM}\Delta\dot{\theta}_m + n_p L\dot{\theta}_{m0}\Delta i_d + n_p L i_{d0}\Delta\dot{\theta}_m] \tag{15.2}$$

The overall system consists of (6), (10), and the variations of (12). It can be written in matrix form in the Laplace domain, formally replacing the time derivative p by the complex variable s:

$$s\cdot\begin{bmatrix}\Delta\psi_d\\ \Delta\psi_q\\ \Delta\dot{\theta}\\ \Delta\varepsilon_{id}\\ \Delta\varepsilon_{iq}\\ \Delta\varepsilon_{\Omega}\end{bmatrix} = [A_{sys}]\begin{bmatrix}\Delta\psi_d\\ \Delta\psi_q\\ \Delta\dot{\theta}\\ \Delta\varepsilon_{id}\\ \Delta\varepsilon_{iq}\\ \Delta\varepsilon_{\Omega}\end{bmatrix} + \begin{bmatrix}1 & 0\\ 0 & 1\\ 0 & 0\\ 0 & 0\\ 0 & 0\\ 0 & 0\end{bmatrix}\begin{bmatrix}v_{d(h)}\\ v_{q(h)}\end{bmatrix} \tag{16}$$

where the system matrix A_{sys} is given in (17).

The system (16) is solved and all the relevant transfer functions relating the inputs $v_{d(h)}$ and $v_{q(h)}$ and the state variables are found. In this analysis, the transfer functions in (18) are particularly important because they define the

$$A_{sys} = \begin{bmatrix} -\frac{R}{L} - \frac{k_{pI}}{L(1+sT_{sw})} & \frac{sT_{sw}}{1+sT_{sw}}\dot{\theta}_0 & \frac{sT_{sw}}{1+sT_{sw}}\psi_{q0} & \frac{k_{iI}}{1+sT_{sw}} & 0 & 0 \\ -\frac{sT_{sw}}{1+sT_{sw}}\dot{\theta}_0 & -\frac{R}{L} - \frac{k_{pI}}{L(1+sT_{sw})} & a_{23}(s) & 0 & \frac{k_{iI}}{1+sT_{sw}} & \frac{k_{pI}k_{i\Omega}}{n_p\psi_{PM}(1+sT_{sw})} \\ 0 & a_{32}(s) & 0 & 0 & 0 & 0 \\ -1/L & 0 & 0 & 0 & 0 & 0 \\ 0 & -1/L & -\frac{k_{p\Omega}}{n_p^2\psi_{PM}} & 0 & 0 & \frac{k_{i\Omega}}{n_p\psi_{PM}} \\ 0 & 0 & -1/n_p & 0 & 0 & 0 \end{bmatrix} \tag{17}$$

$$a_{32}(s) = \frac{\psi_{PM}}{L} n_p^2 \frac{J_L s^2 + Bs + K}{J_m J_L s^2 + B(J_m + J_L)s + K(J_m + J_L)} \text{ and } a_{23}(s) = -\psi_{d0} + \frac{sT_{sw}}{1+sT_{sw}}\psi_{PM} - \frac{k_{pI}k_{p\Omega}}{n_p^2\psi_{PM}(1+sT_{sw})}$$

contributions of the harmonic voltages in the dq-frame to the torque harmonic. Their analytical expressions are given in Appendix II.

$$G_{em,d} = T_{em,h}(s)/V_{dh}(s)\,;\; G_{em,q} = T_{em,h}(s)/V_{qh}(s) \quad (18)$$

Furthermore, the transfer function between the electromagnetic and the shaft torque, obtained from (7), is:

$$\frac{T_{sh,h}(s)}{T_{em,h}(s)} = G_{sh} = \frac{J_L(Bs+K)}{J_m J_L s^2 + (J_m+J_L)(Bs+K)} \quad (19)$$

Therefore, the transfer functions between the voltage harmonics in the dq-frame and the shaft torque harmonic are:

$$G_{sh,d} = \frac{T_{sh,h}(s)}{V_{dh}(s)} = G_{em,d}\cdot G_{sh}; \quad (20.1)$$

$$G_{sh,q} = \frac{T_{sh,h}(s)}{V_{qh}(s)} = G_{em,q}\cdot G_{sh}; \quad (20.2)$$

As an example, let us plot the transfer functions $G_{em,dq}$ and $G_{sh,dq}$ for a system whose data are given in Appendix I. The fundamental frequency is f_1 = 5Hz and $i_{q0} = 0.2I_n$. Two different cases are considered: the first one is characterized by switching frequency f_{sw}=75Hz and current loop bandwidth $f_{c,I}$=1.8Hz much lower than $f_{N,mech}$, while in the second case these values are much higher than $f_{N,mech}$: f_{sw}=5kHz and $f_{c,I}$=300Hz. The speed loop bandwidth is considerably low to avoid instability. The results are given in Fig. 4, where the complex frequency s is treated as a continuous variable, i.e. it is the frequency of the harmonic input $v_{dq(h)}$.

Several conclusions can be made from Fig. 4:

- Regardless of the current loop bandwidth, as the forcing harmonic frequency approaches the mechanical resonant frequency $f_{N,mech}$, the amplitude $T_{em,h}$ decreases significantly, almost becoming null.
- In case of $f_{c,I} << f_{N,mech}$, there is an evident peak in both $T_{em,h}$ and $T_{sh,h}$ at a frequency slightly higher than $f_{N,mech}$: this point defines a new overall resonant frequency f_N. Its value is a root of the denominator polynomial in (18) and for our system f_N = 117Hz. This is not the case with $f_{c,I} >> f_{N,mech}$ because, as expected, the current loop damps the oscillations.
- In both cases, the contribution of $v_{d(h)}$ to the torque magnitudes is less significant with respect to $v_{q(h)}$.

C. Torque harmonic magnitude estimation due to phase voltage harmonic

It is more significant to evaluate the effect of a phase voltage harmonic $\bar{v}_{\alpha\beta(h_v)}$ on the torque harmonic $T_{em,h}$ and consequently $T_{sh,h}$. It can be done in the frequency domain by superposing the effects of $v_{d(h)}$ and $v_{q(h)}$ on the torque amplitudes.

Let us assume a voltage harmonic of positive sequence at frequency $\omega_h = h_v\cdot\omega_1$. Applying the Park transform, the same harmonic in the dq-frame is:

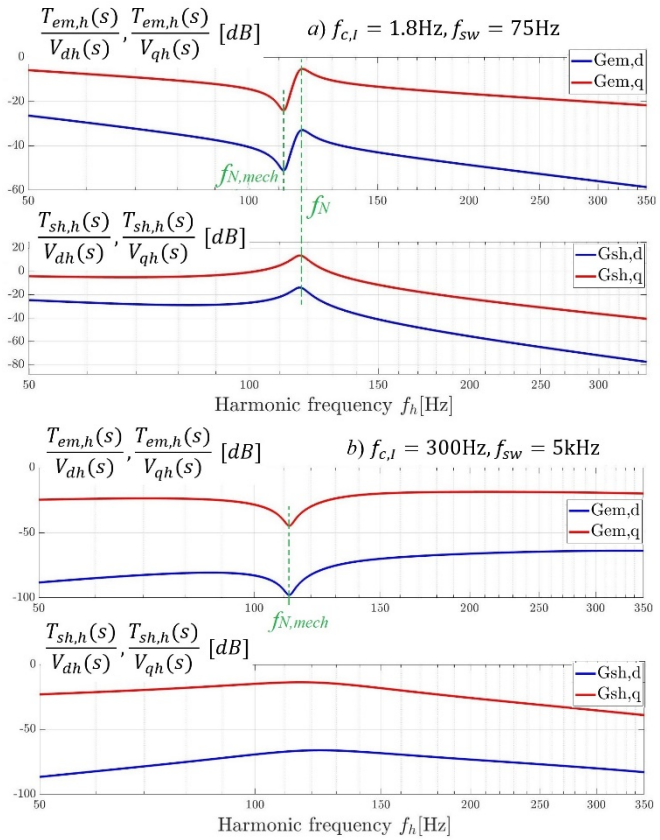

Fig. 4. Bode mag. response to a voltage harmonic. Transfer functions from $v_{d(h)}$, $v_{q(h)}$ to $T_{em,h}$, $T_{sh,h}$: a) $f_{c,I}$ = 1.8Hz, f_{sw} = 75Hz b) $f_{c,I}$ = 300Hz, f_{sw} = 5kHz

$$\begin{cases} v_{d(h)} = \sqrt{3}V_h\, sin(h\omega_1 t) \\ v_{q(h)} = \sqrt{3}V_h\, cos(h\omega_1 t) \end{cases} \quad h = (h_v - 1) \quad (21)$$

By evaluating the amplitudes and the phases of the transfer functions $G_{em,d}$ and $G_{em,q}$ given in (18) at the forcing frequency ω_h and combining them in the frequency domain, the amplitude $T_{em,h}$ can be estimated as [11]:

$$\left|T_{em,h}\right| = \sqrt{3}V_h\sqrt{k_1^2 + k_2^2} \quad (22)$$

where the gains k_1 and k_2 are given in (23). In a similar way, the formula can be obtained for the shaft torque harmonic $T_{sh,h}$, using the transfer functions in (20). The same approach is valid for a negative sequence voltage harmonic as well.

As an example, let us consider h_v=13, which results in a torque harmonic h=12. Keeping the harmonic order fixed and $i_{q0} = 0.2I_n$, the fundamental frequency is varied and the magnitudes $T_{em,h}$ and $T_{sh,h}$ are evaluated in two cases, with current loop bandwidth lower and higher than $f_{N,mech}$, respectively. The switching frequency is $f_{sw}=m_f f_1$, where m_f=15 and m_f=1002, respectively. The results are shown in Fig. 5: the system at each point operates at steady state.

- In both cases, $T_{em,h}$ becomes almost zero when the modulation results in a harmonic at a frequency $f_{N,mech}$.
- At the same time, $T_{sh,h}$ starts increasing.

$$k_1 = \left|G_{em,d}(j\omega_h)\right| cos\left(arg\left(G_{em,d}(j\omega_h)\right)\right) - \left|G_{em,q}(j\omega_h)\right| sin\left(arg\left(G_{em,q}(j\omega_h)\right)\right) \quad (23.1)$$

$$k_2 = \left|G_{em,d}(j\omega_h)\right| sin\left(arg\left(G_{em,d}(j\omega_h)\right)\right) + \left|G_{em,q}(j\omega_h)\right| cos\left(arg\left(G_{em,q}(j\omega_h)\right)\right) \quad (23.2)$$

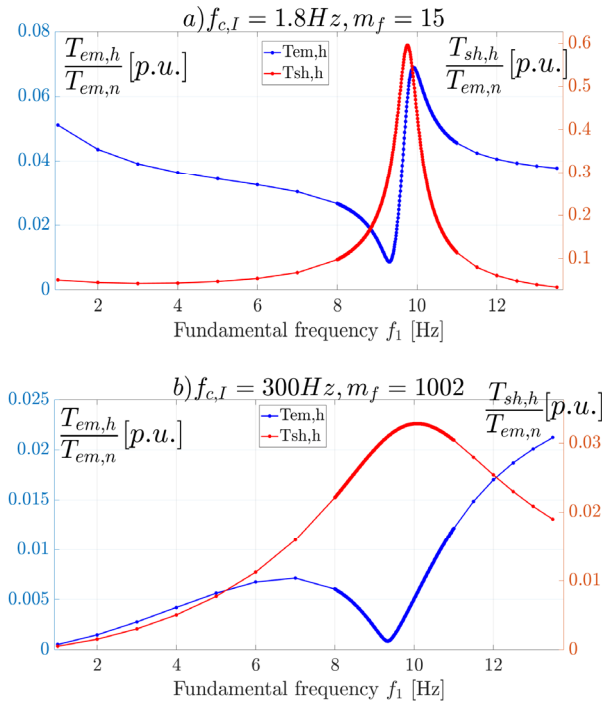

Fig. 5. Amplitude of the electromagnetic $T_{em,h}$ and shaft torque $T_{sh,h}$ harmonics due to a phase voltage harmonic. a) $f_{c,I}$ = 1.8Hz, m_f=15 b) $f_{c,I}$ = 300Hz, m_f=1002.

- With $f_{c,I} << f_{N,mech}$, both $T_{em,h}$ and $T_{sh,h}$ have a peak value when f_h=f_N.
- With $f_{c,I} >> f_{N,mech}$ only $T_{sh,h}$ reaches a peak value at f_h=f_N and its value is much lower than in the case with low current loop bandwidth.

IV. Validation by Simulation

As a first step, the transfer functions $G_{em,dq}$ and $G_{sh,dq}$ obtained in (18) and (20) were verified in Matlab/Simulink. All the PMSM drive parameters are given in Appendix II. At fixed fundamental f_1=5Hz, sinusoidal perturbations $v_{d(h)}$ and $v_{q(h)}$ with variable harmonic h were injected. Two cases were considered, both with i_{q0} = 0.2I_n: current loop bandwidth lower and higher than the mechanical torsional frequency, respectively. The results are shown in Fig. 6.

It can be noticed that in case of current loop bandwidth lower than $f_{N,mech}$ the analytical results match perfectly the simulation values. In case of current bandwidth higher than $f_{N,mech}$ instead, there is an apparent discrepancy between the computed and simulated results related to the d-axis transfer functions. This outcome can be explained by the numerically low values of about -70dB in Fig. 6b). Therefore, it is not necessary to insist on lowering the mismatch.

As explained in Section IV, predicting correctly the amplitude of the electromagnetic and the shaft torque harmonic due to a harmonic voltage is more important than the individual transfer functions. Let us consider a voltage harmonic h_v=13 which excites the h=12th torque harmonic. Varying the fundamental frequency f_1, i.e. varying the drive operating speed, torque amplitudes were estimated both analytically and in Simulink. The results in case of significantly different values for the current loop bandwidth

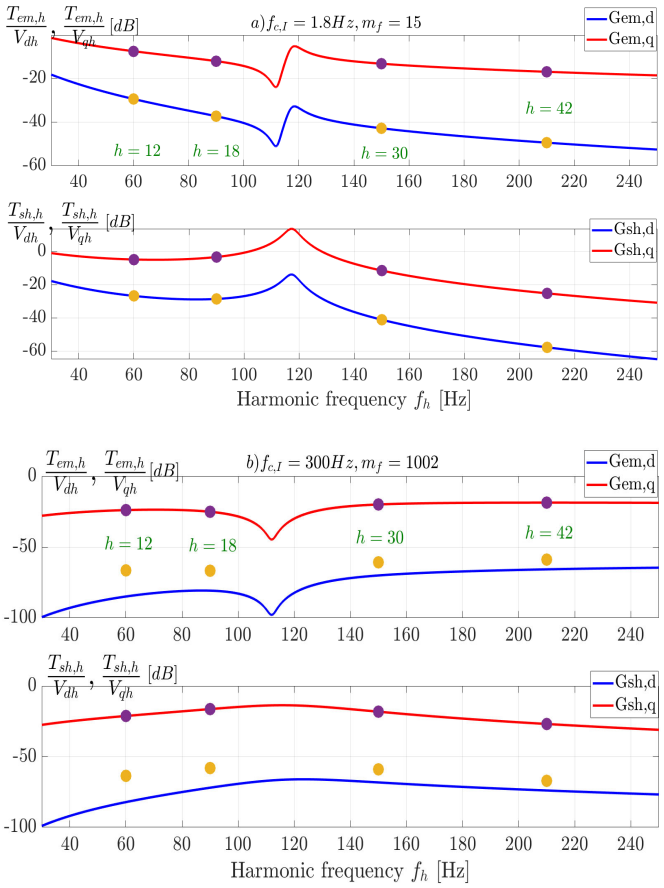

Fig. 6. Transfer functions between inputs $v_{d(h)}$ and $v_{q(h)}$ and outputs $T_{em,h}$ and $T_{sh,h}$ for fixed f_1 and variable harmonic frequency. Comparison between analytical (full lines) and simulated results (points) for two different cases: a) $f_{c,I}$ = 1.8Hz, m_f=15 b) $f_{c,I}$ = 300Hz, m_f=1002.

are shown in Fig. 7 and Fig. 8.

In both cases, the analytical results are aligned with the simulation ones. It means the analytical model predicts accurately the torque amplitudes. Even though there was a little discrepancy between the analytical d-axis transfer function values and the simulation outcome, both T_{em} and T_{sh} harmonics are predicted correctly since the q-axis quantities have a much more significant effect on the torque responses, due to the PMSM principle of operation. Having enhanced our understanding of how the overall system responds in/around resonance, these findings will help to prevent from system damage due to torsional vibrations.

V. Conclusion

A mathematical model of an electric drive containing a PMSM and operating in/around torsional resonance was presented in this paper. The model accounted for electrical, mechanical, and control aspects through suitable differential equations. On-hand formulae for predicting analytically the amplitude of the electromagnetic and the shaft torque harmonic were obtained. The resulting analytical solution gave an insight of the interconnections between various drive aspects. The results were verified through extensive simulations.

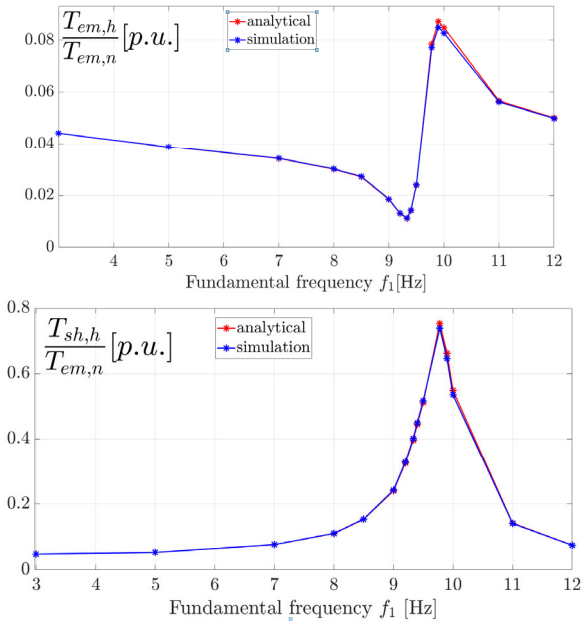

Fig. 7. Amplitude of the electromagnetic $T_{em,h}$ and the shaft torque $T_{sh,h}$ harmonic in case of current loop bandwidth $f_{c,I}$ = 1.8Hz << $f_{N,mech}$. Comparison between analytical and simulation results.

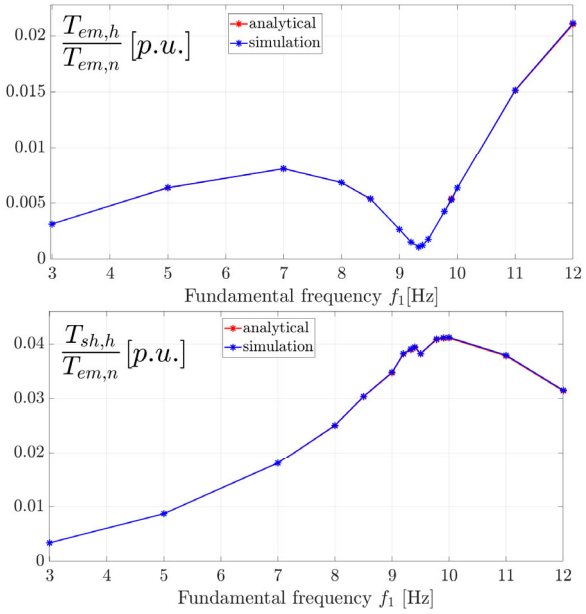

Fig. 8. Amplitude of the electromagnetic $T_{em,h}$ and the shaft torque $T_{sh,h}$ harmonic in case of current loop bandwidth $f_{c,I}$ = 300Hz >> $f_{N,mech}$. Comparison between analytical and simulation results.

VI. References

[1] M. Brunelli, A. Fusi, F. Grasso, F. Pasteur, A. Ussi, "Torsional vibration analysis of reciprocating compressor trains driven by induction motors", 9th International conference on compressors and their systems, 2015, pp. 1-10.

[2] J. Song-Manguelle, G. Ekemb, D. L. Mon-Nzongo, T. Jin and M. L. Doumbia, "A theoretical analysis of pulsating torque components in ac machines with variable frequency drives and dynamic mechanical loads," IEEE Trans. on Industrial Electronics, vol. 65, no. 12, pp. 9311-9324, Dec. 2018.

[3] R. M. Pindoriya, R. K. Thakrur, B. S. Rajpurohit, R. Kumar, "Numerical and experimental analysis of torsional vibration and acoustic noise of PMSM coupled with dc generator", IEEE Transactions on Industrial Electronics, Vol. 69, Iss. 4, April 2022.

[4] J. Hu, T. Peng, M. Jia, Y. Yang, Y. Guan, "Study on electromechanical coupling characteristics of an integrated electric drive system for electric vehicle", IEEE Access, Vol. 7, Nov. 2019, pp.166493-166508.

[5] Ch. Xia, B. Ji, Y. Yan, "Smooth speed control for low-speed nigh-torque permanent-magnet synchronous motor using proportional-integral-resonant converter", IEEE Transactions on Industrial electronics, Vol. 62, No. 4, April 2015, pp.2123-2134.

[6] Q. Wang, T. D. Feese, B. C. Pettinato, "Torsional natural frequencies: measurement vs. prediction", Proceedings of the 41st Turbomachinery Symposium, Houston, Texas, 24-27 September 2012, pp. 1-32.

[7] M. Bruha, "Electro-mechanical interaction between electric drive and its mechanical load and control interventions mitigating unwanted vibration phenomena," Ph.D. dissertation, Faculty of Electr. Engin., Univ. of West Bohemia, Pilsen, Czech Republic, 2018.

[8] S. Thomsen, N. Hoffmann, F. W. Fuchs, "PI control, PI-based state space control, and model-based predictive control for drive systems with elastically coupled loads – a comparative study", IEEE Trans. On Industrial Electronics, Vol. 58, No. 8, August 2011, pp. 3647-3656.

[9] M. A. Valenzuela, J. M. Bentley, B. D. Lorenz, "Evaluation of torsional oscillations in paper machine sections", IEEE Transactions on Industrial Applications, Vol. 41, No. 2, March 2005, pp. 493-501.

[10] S. E. Saarakkala, M. Hinkkanen, "State-Space speed control of two-mass mechanical systems: analytical tuning and experimental validation", IEEE Trans. on Industry Applications, Vol. 50, No. 5, Sept./Oct. 2014, pp. 3428-3437.

[11] D. Pejovski, A. Di Gerlando, G. M. Foglia, R. Perini, "Analytical model of Permanent Magnet Synchronous Machine in/around Resonance", submitted to XXV International Conference on Electrical Machines, Valencia, Spain, 5-8 Sept. 2022.

VII. Biographies

Dejan Pejovski received his MS degree in electrical engineering at Politecnico di Milano, Milano, Italy in 2019. Currently, he is a PhD student in Electrical Engineering at Politecnico di Milano. His interests are in power electronics, electrical machines and drives.

Antonino Di Gerlando received his MS degree in electrical engineering from the Politecnico di Milano, Italy, in 1981. Currently, he is a Full Professor at the Department of Energy at Politecnico di Milano. Fields of interest: design and modelling of electrical machines, converters and drive systems. He is a senior member of IEEE, and member of the Italian Association AEIT.

Giovanni Maria Foglia received his MS degree and the PhD in electrical engineering from the Politecnico di Milano, Milano, Italy, in 1997 and 2000. Currently, he is an Assistant Professor at the Department of Energy at Politecnico di Milano, and his main field of interest is the analysis and design of PM electrical machines.

Roberto Perini (M'10) received his MS degree and the PhD in electrical engineering from the Politecnico di Milano, Milano, Italy. Currently, he is an Associate Professor at the Department of Energy at Politecnico di Milano. His interests are in the design and modelling of electrical machines and power electronics.

VIII. Appendix I

TABLE I
PMSM, Load, Coupling and Control System Data

Rated power P_n [kW]	6.91
Rated torque $T_{em,n}$ [Nm]	22
Number of pole pairs n_p	3
Rated frequency f_n [Hz]	150
Permanent magnet flux Ψ_{PM} [Wb]	0.165
Phase resistance R [Ω]	0.393
Synchronous inductance L_d=L_q=L [H]	$4.8 \cdot 10^{-3}$
Motor side inertia J_m [kg·m^2]	$3 \cdot 10^{-3}$
Load side inertia J_L [kg·m^2]	$123 \cdot 10^{-3}$
Coupling stiffness K [Nm/rad]	1458.5
Coupling damping B [Nms/rad]	0.0567
Proportional coeff. of the current regulator k_{pI} [V/A]	0.045 / 9.473
Integral coeff. of the current regulator k_{iI} [Vrad/As]	0.475 / 3740
Proportional coeff. of the speed reg. $k_{pΩ}$ [Nms/rad]	0.134 / 0.776
Integral coeff. of the speed regulator $k_{iΩ}$ [Nm]	0.145 / 0.857

IX. APPENDIX II

$$G_{em,d}(s) = \frac{T_{em,h}(s)}{V_{dh}(s)} = \frac{G_{em,d}^{num}(s)}{G_{em,d}^{den}(s)};\ G_{em,q} = \frac{T_{em,h}(s)}{V_{qh}(s)} = \frac{G_{em,q}^{num}(s)}{G_{em,q}^{den}(s)}$$

$$G_{em,d}^{num}(s) = -J_m J_L L n_p \psi_{PM} s^5 (s + T_{sw}^{-1})\dot{\theta}_0 \left[s^2 + \omega_{N,mech}^2 \left(\frac{Bs}{K} + 1\right)\right]$$

$$G_{em,q}^{num}(s) = J_m J_L n_p \psi_{PM} s^3 (s + T_{sw}^{-1}) \left[s^2 + \omega_{N,mech}^2 \left(\frac{Bs}{K} + 1\right)\right] \left[s(R + sL)(s + T_{sw}^{-1}) + (sk_{pI} + k_{iI})T_{sw}^{-1}\right]$$

$$G_{em,dq}^{den}(s) = a_{10}s^{10} + a_9 s^9 + \cdots + a_1 s + a_0$$

$$a_{10} = J_m J_L L^2$$

$$a_9 = (J_m + J_L)BL^2 + 2J_m J_L L(LT_{sw}^{-1} + R)$$

$$a_8 = J_L L\left(n_p \psi_{PM}\right)^2 + (J_m + J_L)[KL + 2B(LT_{sw}^{-1} + R)]L + J_m J_L \left((LT_{sw}^{-1})^2 + R^2 + 2L\left(k_{pI} + 2R\right)T_{sw}^{-1} + \left(\dot{\theta}_0 L\right)^2\right)$$

$$\begin{aligned} a_7 = {} & J_L k_{pI} k_{p\Omega} L T_{sw}^{-1} + \left(n_p \psi_{PM}\right)^2 [BL + J_L(LT_{sw}^{-1} + R)] + J_m J_L 2\left[k_{iI} L + \left(k_{pI} + R\right)(LT_{sw}^{-1} + R)\right]T_{sw}^{-1} \\ & + (J_m + J_L)\left\{2KL(LT_{sw}^{-1} + R) + B\left[(LT_{sw}^{-1})^2 + R^2 + 2L\left(k_{pI} + 2R\right)T_{sw}^{-1} + \left(\dot{\theta}_0 L\right)^2\right]\right\} + i_{q0} J_L L^2 n_p^2 \psi_{PM} \dot{\theta}_0 \end{aligned}$$

$$\begin{aligned} a_6 = {} & \left[J_L L\left(k_{pI} k_{i\Omega} + k_{iI} k_{p\Omega} + k_{pI} k_{p\Omega} T_{sw}^{-1}\right) + k_{pI} k_{p\Omega}(BL + J_L R)\right]T_{sw}^{-1} \\ & + \left(n_p \psi_{PM}\right)^2 \left[J_L\left(k_{pI} + R\right)T_{sw}^{-1} + L(BT_{sw}^{-1} + K) + BR\right] + J_m J_L \left[2k_{iI} R + \left(2k_{iI} L + \left(k_{pI} + R\right)^2\right)T_{sw}^{-1}\right]T_{sw}^{-1} \\ & + B i_{q0} L^2 n_p^2 \psi_{PM} \dot{\theta}_0 \\ & + (J_m + J_L)\left\{2B\left[k_{iI} L + \left(k_{pI} + R\right)(LT_{sw}^{-1} + R)\right]T_{sw}^{-1}\right. \\ & \left. + K\left[(LT_{sw}^{-1})^2 + R^2 + 2L\left(k_{pI} + 2R\right)T_{sw}^{-1} + \left(\dot{\theta}_0 L\right)^2\right]\right\} \end{aligned}$$

$$\begin{aligned} a_5 = {} & T_{sw}^{-1}\left\{J_L k_{pI} k_{p\Omega}\left(k_{pI} + R\right)T_{sw}^{-1} + L\left[J_L k_{iI} k_{i\Omega} + K k_{pI} k_{p\Omega} + B\left(k_{pI} k_{i\Omega} + k_{iI} k_{p\Omega}\right)\right]\right. \\ & + (LT_{sw}^{-1} + R)\left(Bk_{pI} k_{p\Omega} + J_L k_{iI} k_{p\Omega} T_{sw}^{-1} + J_L k_{pI} k_{i\Omega}\right) \\ & + \left(n_p \psi_{PM}\right)^2 \left[B\left(k_{pI} + R\right)T_{sw}^{-1} + K(LT_{sw}^{-1} + R) + J_L k_{iI} T_{sw}^{-1}\right] + 2k_{iI} J_m J_L \left(k_{pI} + R\right)T_{sw}^{-1} \\ & + (J_m + J_L)\left[2Kk_{iI} L + 2Bk_{iI} R + 2K\left(k_{pI} + R\right)(LT_{sw}^{-1} + R) + B\left(2k_{iI} L + \left(k_{pI} + R\right)^2\right)T_{sw}^{-1}\right]\Big\} \\ & + i_{q0} KL^2 n_p^2 \psi_{PM} \dot{\theta}_0 \end{aligned}$$

$$\begin{aligned} a_4 = {} & T_{sw}^{-1}\left\{L\left[k_{iI}\left(Bk_{i\Omega} + Kk_{p\Omega}\right) + Kk_{pI} k_{i\Omega}\right] + R\left[k_{iI}\left(J_L k_{i\Omega} + Bk_{p\Omega}\right) + k_{pI}\left(Bk_{i\Omega} + Kk_{p\Omega}\right)\right]\right. \\ & + T_{sw}^{-1}\left[Kk_{pI} k_{p\Omega} L + B\left(k_{pI}\left(k_{pI} k_{p\Omega} + k_{i\Omega} L\right) + k_{p\Omega}\left(k_{iI} L + k_{pI} R\right)\right)\right. \\ & \left. + J_L\left(k_{iI} k_{i\Omega} L + k_{pI} k_{i\Omega}\left(k_{pI} + R\right) + k_{iI} k_{p\Omega}\left(2k_{pI} + R\right)\right)\right] + \left(n_p \psi_{PM}\right)^2 \left[Bk_{iI} + K\left(k_{pI} + R\right)\right] \\ & + J_L J_m T_{sw}^{-1} k_{iI}^2 + (J_m + J_L)\left[2KRk_{iI} + 2Bk_{iI}\left(k_{pI} + R\right)T_{sw}^{-1} + K\left(2k_{iI} L + \left(k_{pI} + R\right)^2\right)T_{sw}^{-1}\right]\Big\} \end{aligned}$$

$$\begin{aligned} a_3 = {} & T_{sw}^{-1}\left\{BT_{sw}^{-1}\left[k_{pI}^2 k_{i\Omega} + k_{iI}\left(2k_{pI} k_{p\Omega} + k_{i\Omega} L + k_{iI}(J_m + J_L)\right)\right] + KRk_{pI} k_{i\Omega} + BR\left[k_{pI} k_{i\Omega} T_{sw}^{-1} + k_{iI}\left(k_{i\Omega} + k_{p\Omega} T_{sw}^{-1}\right)\right]\right. \\ & + Kk_{iI}\left(k_{i\Omega} L + \left(n_p \psi_{PM}\right)^2 + k_{p\Omega} R\right) + J_L k_{iI}\left[2k_{pI} k_{i\Omega} + k_{iI} k_{p\Omega} + k_{i\Omega} R + 2K\left(k_{pI} + R\right)\right]T_{sw}^{-1} \\ & \left. + K\left[k_{pI}^2 k_{p\Omega} + k_{pI} k_{i\Omega} L + k_{iI} k_{p\Omega} L + k_{pI} k_{p\Omega} R + 2J_m k_{iI}\left(k_{pI} + R\right)\right]T_{sw}^{-1}\right\} \end{aligned}$$

$$\begin{aligned} a_2 = {} & T_{sw}^{-1}\left\{k_{iI} k_{i\Omega} KR\right. \\ & + \left[k_{iI}\left(Bk_{i\Omega} + Kk_{p\Omega}\right)\left(2k_{pI} + R\right) + Kk_{i\Omega}\left(k_{pI}\left(k_{pI} + R\right) + k_{iI} L\right)\right. \\ & \left. \left. + k_{iI}^2\left((J_m + J_L)K + J_L k_{i\Omega} + Bk_{p\Omega}\right)\right]T_{sw}^{-1}\right\} \end{aligned}$$

$$a_1 = k_{iI}\left[k_{iI}\left(Bk_{i\Omega} + Kk_{p\Omega}\right) + Kk_{i\Omega}\left(2k_{pI} + R\right)\right]T_{sw}^{-2}$$

$$a_0 = Kk_{iI}^2 k_{i\Omega} T_{sw}^{-2}$$

$$\omega_{N,mech}^2 = \frac{K(J_m + J_L)}{J_m J_L}$$